Dissociation products and structures of solid H_2S at strong compression

Yinwei Li,[1] Lin Wang,[2,3] Hanyu Liu,[3,4] Yunwei Zhang,[3] Jian Hao,[1] Chris J. Pickard,[5] Joseph R. Nelson,[6] Richard J. Needs,[6] Wentao Li,[2] Yanwei Huang,[2] Ion Errea,[7,8] Matteo Calandra,[9] Francesco Mauri,[9] and Yanming Ma[3,*]

[1]*School of Physics and Electronic Engineering, Jiangsu Normal University, Xuzhou 221116, China*
[2]*Center for High Pressure Science and Technology Advanced Research, Shanghai, 201203, China*
[3]*State Key Laboratory of Superhard Materials, Jilin University, Changchun 130012, China*
[4]*Geophysical Laboratory, Carnegie Institution of Washington, Washington D.C. 20015, USA*
[5]*Department of Materials Science & Metallurgy, University of Cambridge, 27 Charles Babbage Road, Cambridge CB3 0FS, United Kingdom*
[6]*Theory of Condensed Matter Group, Cavendish Laboratory, J J Thomson Avenue, Cambridge CB3 0HE, United Kingdom*
[7]*Donostia International Physics Center (DIPC), Manuel de Lardizabal pasealekua 4, 20018 Donostia-San Sebastián, Basque Country, Spain*
[8]*Fisika Aplikatua 1 Saila, EUITI Bilbao, University of the Basque Country (UPV/EHU), Rafael Moreno "Pitxitxi" Pasealekua 3, 48013 Bilbao, Basque Country, Spain*
[9]*IMPMC, UMR CNRS 7590, Sorbonne Universités - UPMC Univ. Paris 06, MNHN, IRD, 4 Place Jussieu, F-75005 Paris, France*

Hydrogen sulfides have recently received a great deal of interest due to the record high superconducting temperatures of up to 203 K observed on strong compression of dihydrogen sulfide (H_2S). A joint theoretical and experimental study is presented in which decomposition products and structures of compressed H_2S are characterized, and their superconducting properties are calculated. In addition to the experimentally known H_2S and H_3S phases, our first-principles structure searches have identified several energetically competitive stoichiometries that have not been reported previously; H_2S_3, H_3S_2, and H_4S_3. In particular, H_4S_3 is predicted to be thermodynamically stable within a large pressure range of 25–113 GPa. High-pressure room-temperature X-ray diffraction measurements confirm the presence of H_3S and H_4S_3 through decomposition of H_2S that emerge at 27 GPa and coexist with residual H_2S, at least up to the highest pressure studied in our experiments of 140 GPa. Electron-phonon coupling calculations show that H_4S_3 has a small T_c of below 2 K, and that H_2S is mainly responsible for the observed superconductivity of samples prepared at low temperature (<100K).

PACS numbers: 62.50.-p, 61.50.Ah, 61.05.cp, 74.70.Ad

Superconductivity with a transition temperature T_c of up to 203 K was observed recently in solid H_2S at Megabar pressures, which is the highest record among all known superconductors [1]. Ashcroft suggested that metallic hydrogen would be a superconductor at high pressures with a T_c around room temperature [2], and subsequently predicted that hydrogen-rich metallic compounds might also be superconducting at high pressures [3]. Early theoretical studies focussed on high-pressure silicon and aluminum hydrides [4, 5], and a number of potential high-temperature superconductors have now been proposed in compressed hydrogen-rich compounds, with T_cs estimated in the range 40–250 K (e.g., GaH_3 [6, 7], SnH_4 [8], GeH_4 [9], NbH_4 [10], Si_2H_6 [11], $SiH_4(H_2)_2$ [12], CaH_6 [13], YH_3 [14], YH_4 and YH_6 [15]). They have not been realized in practice, in part because of demanding experimental challenges.

The high pressure phase diagram of H_2S has been studied extensively. H_2S is a sister molecule of H_2O, and is the only known stable compound in the H-S system at ambient pressure. High-pressure diamond anvil cell experiments led to the discovery of a metallic phase at about 96 GPa [16–27]. However, partial decomposition of H_2S and elemental sulfur was observed in Raman [26] and XRD studies [21] at room temperature above 27 GPa. H_2S had not been considered as a candidate for superconductivity because it was believed to dissociate into elemental sulfur and hydrogen under high pressures [28]. Recent first-principles structure searches predicted energetically stable metallic structures of H_2S above 110 GPa [29] and excluded dissociation into its elements. An estimated maximum T_c for metallic H_2S of 80 K at 160 GPa was predicted [29]. Motivated by this study, Drozdov *et al.* [1] performed high-pressure experiments on solid H_2S looking for superconductivity and found an astonishing T_c of 203 K at 155 GPa [1]. H_2S shows complex superconducting behavior at high pressures with the emergence of two different superconducting states. Samples prepared at low temperature (100 K) have a T_c of ∼30 K at 110 GPa at the onset of superconductivity, which increases rapidly to a maximum value of 150 K at 200 GPa, while samples at room temperature or above show a maximum T_c of 203 K at 155 GPa.

Strobel *et al.* synthesized another H-S compound, H_3S, by compressing a mixture of H_2S and H_2 above 3.5 GPa [30]. The superconducting T_c of H_3S at 200 GPa was recently predicted to be as high as 191–204 K [31], with H_3S in a cubic $Im\bar{3}m$ structure, which is known already

in H_3O at terapascal pressures [32] through decomposition of H_2O. The agreement between experimental [1] and theoretical values of T_c [31] led to the proposal by Drozdov *et al.* that H_3S could be formed by decomposition of H_2S and might be responsible for the observed superconducting state at 203 K [1]. This proposal was supported by first-principles density-functional-theory (DFT) studies which suggested that it is thermodynamically favorable for H_2S to decompose into H_3S + S [33–35] at pressures above 43 GPa [34]. Apparently, there is an urgent need to characterize the decomposition products of compressed H_2S in an effort to build an understanding of the complex superconducting behavior exhibited by the H-S system.

Here we present a joint theoretical and experimental study of compressed H_2S which clarifies the possible decomposition products and their structures. First-principles DFT structure searches were used to predict several new stoichiometries (H_2S_3, H_3S_2, and H_4S_3) and a new structure in H_3S not reported previously. Room-temperature high pressure X-ray diffraction (XRD) experiments demonstrate that above 27 GPa, H_2S partially decomposes into S + H_3S + H_4S_3. H_4S_3 emerges as the major component at around 66 GPa and coexists with a small fraction of H_3S and residual H_2S, at least up to the highest pressure studied experimentally of 140 GPa.

Extensive structure searches over 44 H-S stoichiometries at 25, 50, 100 and 150 GPa were performed using the CALYPSO [36, 37] and AIRSS [4, 38] methods, which have been successfully used to investigate structures of materials at high pressures [4, 13, 39–45]. The underlying structural relaxations were performed using the Vienna *ab initio* simulation package (VASP) [46] for CALYPSO and the CASTEP plane-wave code [47] for AIRSS. Electron-phonon coupling (EPC) calculations were performed with density functional perturbation theory using the Quantum-ESPRESSO package[48]. XRD data were collected at the 15U1 beamline at the Shanghai Synchrotron Radiation Facility (SSRF) with a monochromatic beam of wavelength 0.6199 Å. The diffraction patterns were integrated with the FIT2D computer code [49] and fitted by Rietveld profile matching using the GSAS+EXPGUI programs [50, 51]. More information about the calculations and experiments is provided in the Supplemental Material [52].

Figure 1 shows convex hull diagrams at 25, 50, 100 and 150 GPa which summarize the results of the structure searches. The effects of including quantum zero-point vibrational motion are significant and they tend to increase with pressure. Our results suggest that up to five H-S compounds lie on the convex hull at some pressures and are therefore thermodynamically stable. Besides the experimentally known H_2S and H_3S compounds, we predict three additional stable compounds: H_4S_3, H_3S_2 and H_2S_3. Note that H_2S is theoretically found to be stable only below 25 GPa, while H_3S appears at all pressures considered. Enthalpy calculations show that H_3S becomes energetically more stable than H_2S+1/2H_2 at around 6 GPa. The newly predicted H_3S_2 and H_2S_3 phases have very narrow pressure ranges of stability and are unstable above 34 and 25 GPa, respectively (Supplemental Material, Fig. S1 [52]). We have therefore omitted further discussion of these compounds. The corresponding crystallographic parameters and phonon dispersion curves are provided in the Supplemental Material [52].

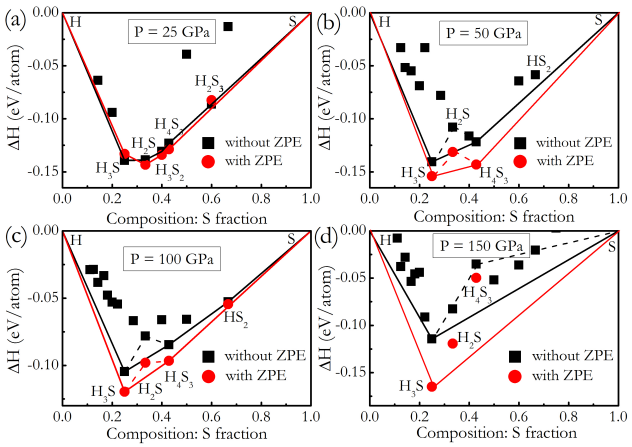

FIG. 1: (Color online) Results from structure searching at 25 (a), 50 (b), 100 (c) and 150 GPa (d). Convex hulls are shown as continuous lines, with (red) and without (black) the inclusion of zero point vibrational enthalpy (ZPE).

For H_3S, besides the P1, Cccm, R3m and Im$\bar{3}$m structures of earlier studies [31], our searches predict a monoclinic C2/c structure (4 f.u/cell) that was not reported earlier. The C2/c structure consists of weakly bonded H_2S and H_2 molecules (Supplemental Material, Fig. S7b [52]), and is calculated to be more stable at pressures of 2–112 GPa than the Cccm structure proposed previously [31] (Supplemental Material, Fig. S7a [52]). Static-lattice enthalpy calculations give a zero-temperature phase sequence for H_3S of P1 → C2/c (2 GPa) → R3m (112 GPa) → Im$\bar{3}$m (180 GPa).

H_4S_3 adopts an orthorhombic $P2_12_12_1$ (4 f.u./cell) structure that consists of weakly bonded HS and H_2S molecules at 25 GPa (Fig. 2a). The H-S bond lengths within the HS and H_2S molecules are 1.354 Å and 1.387-1.391 Å, respectively, which are significantly shorter than the H-S separation of 1.913-1.932 Å between molecules. With increasing pressure, the neighboring molecules bond with each other forming planar H-S-H-S zigzag chains and puckered H-S-H-S chains, respectively. $P2_12_12_1$ transforms to a Pnma structure at 60 GPa (Fig. 2c). The convex hull data suggests two synthesis routes for H_4S_3: (i) decomposition of 8H_2S→S + 4H_3S + H_4S_3 above 25 GPa; (ii) reaction of 4H_3S + 5S → 3H_4S_3 in the pressure range of 25–113 GPa. Theo-

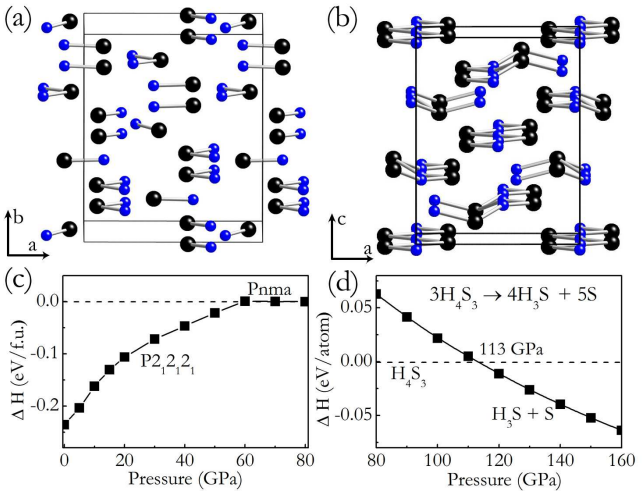

FIG. 2: (Color online) Energetically favorable structures of H_4S_3 with space groups $P2_12_12_1$ (a) and Pnma (b). Small and large spheres represent H and S atoms, respectively. (c) Calculated enthalpy curves of the $P2_12_12_1$ structure with respect to the Pnma structure for H_4S_3 as a function of pressure. (d) Decomposition enthalpy curves of H_4S_3 into (H_3S+S) as a function of pressure.

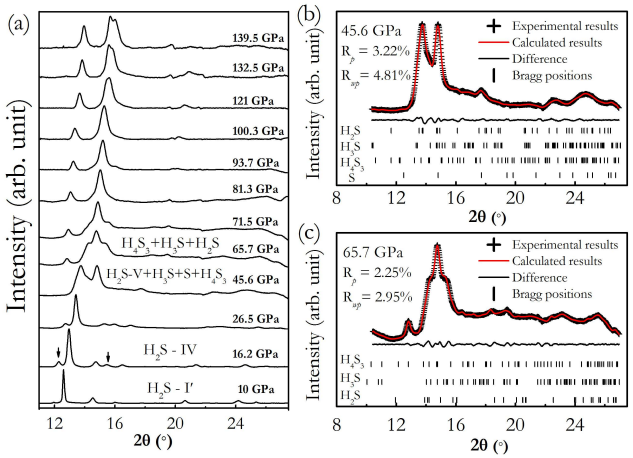

FIG. 3: (Color online) (a) XRD patterns of H_2S collected at various pressures and at room temperature with an incident wavelength of 0.6199 Å. [(b) and (c)] Rietveld refinements of XRD profiles at 45.6 GPa based on the compositions Pc-H_2S, I4$_1$/acd-S, C2/c-H_3S and $P2_12_12_1$-H_4S_3 with phase fractions of 1147:85:31:1, and at 65.7 GPa based on compositions of Pnma-H_4S_3, C2/c-H_3S and Pc-H_2S with phase fractions of 5:3.4:1, respectively. The cross symbols and red solid lines represent observed and fitted patterns, respectively. The solid lines at the bottom are the difference between the observed and fitted patterns. Vertical bars under the pattern represent the calculated positions of reflections arising from the compositions.

retically, it is found that H_4S_3 decomposes into H_3S + S above 113 GPa (Fig. 1d and Fig. 2d).

Powder XRD patterns obtained on increasing pressure from 10 to 140 GPa at room temperature are shown in Fig. 3a. The XRD patterns collected at pressures up to 46 GPa are in excellent agreement with previous data [17–21], and the successive transitions of phase I′ → phase IV → phase V are well reproduced. The XRD data at 10 GPa correspond to phase I′. Phase IV with additional peaks at around 12° and 15° (shown by arrows in Fig. 3a) was observed at 16 GPa. The diffraction peaks of phase IV weaken at pressures above 27 GPa, and a new diffraction profile observed at 46 GPa is responsible for phase V. The XRD data show that the IV→V transition begins above 27 GPa, in excellent agreement with previous results [18, 21].

Previous high-pressure Raman [26] and XRD [21] studies have claimed that decomposition of H_2S occurs at room temperature above 27 GPa. Indeed, we found that H_2S partially decomposes in phase V. Unfortunately, we have not found it possible to resolve the decomposition products and their crystal structures from our current XRD data. Therefore we use the predicted structures and convex hull data to help in analysing the experimental data. At 50 GPa, our calculations suggest an energetically allowed dissociation path of $8H_2S \rightarrow S + 4H_3S + H_4S_3$ (Fig. 1b). The XRD profile at 46 GPa was therefore fitted to a mixture of H_2S + S + H_3S + H_4S_3 by performing Rietveld refinements using the most energetically stable structures. Remarkably, we found that the XRD profile can be well indexed by a mixture of Pc-structured H_2S, I4$_1$/acd-structured S, C2/c-structured H_3S and $P2_12_12_1$-structured H_4S_3, with phase fractions (ratios of numbers of unit cells) of 1147:85:31:1, as shown in Fig. 3b. The existence of a large proportion of H_2S demonstrates the partial decomposition. We also attempted other Rietveld refinements fitting the XRD patterns to pure H_2S, H_2S + S + H_3S or S + $4H_3S$ + H_4S_3, but all of these fits gave poorer results (Supplemental Material, Fig. S10 [46]). The calculated decomposition pressure (30 GPa) for $8H_2S \rightarrow S + 4H_3S + H_4S_3$ (Supplemental Material, Fig. S13 [52]) is in excellent agreement with the value of 27 GPa observed in experiment [21].

With increasing pressure, more H_2S decomposes and its contribution to the XRD signal is reduced. The XRD pattern collected at 66 GPa shows entirely different features to that at 46 GPa. Rietveld refinement shows that a mixture of Pnma-structured H_4S_3, C2/c-structured H_3S, and Pc-structured H_2S with phase fractions 5:3.4:1 gives the best fit to the experimental data (Fig. 3c). The disappearance of elemental S and the reduction in the ratio of H_3S are understandable since a reaction of $4H_3S$ + $5S \rightarrow 3H_4S_3$ takes place as inferred from our convex hull calculations (Fig. 1b and 1c). The two shoulders on the main peak at 15° originate primarily from H_3S and H_2S. These shoulders weaken when the pressure is increased

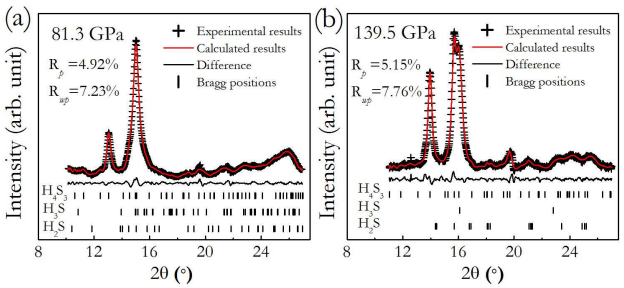

FIG. 4: (Color online) Rietveld refinements of XRD profiles at 81.3 GPa based on Pnma-H_4S_3 + C2/c-H_3S + $Pmc2_1$-H_2S with phase fractions of 43:6:1 (a) and at 139.5 GPa based on Pnma-H_4S_3 + R3m-H_3S + P-1-H_2S with phase fractions of 56:7:1 (c).

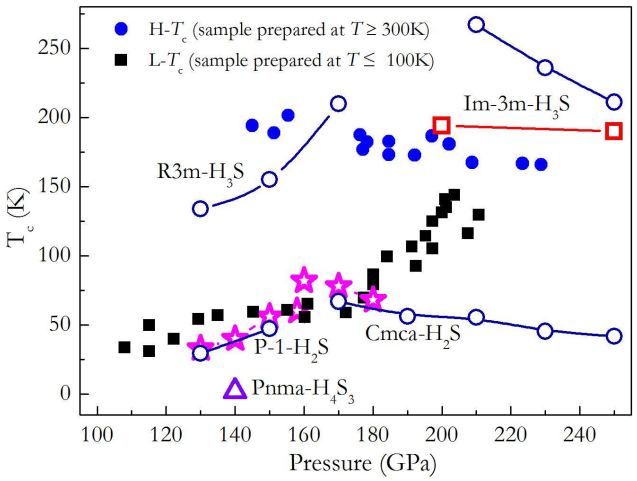

FIG. 5: (Color online) Superconducting transition temperatures (T_c) calculated for various H-S compounds and experimental values for compressed H_2S [1]. Solid squares and circles show experimental data from Fig. 1(b) and Fig. 2 (b) of Ref. 1, respectively, where different runs are represented by the same symbols. The open stars, squares and circles show calculated data from Ref. 29, Ref. 35 and Ref. 54, respectively. Open triangles denote calculated T_c for Pnma-H_4S_3 in the present study. Note that the T_c values (open squares) for Im$\bar{3}$m-H_3S taken from Ref. 35 include anharmonic effects, while all other estimated T_cs are calculated within the harmonic approximation.

to 82 GPa and the XRD pattern can then be well indexed by Pnma-structured H_4S_3, C2/c-structured H_3S and $Pmc2_1$-structured H_2S with a major contribution (86%) from H_4S_3 (Fig. 4a). Our results demonstrate that H_4S_3 coexists with H_3S and H_2S at least up to 140 GPa, the highest pressure studied experimentally (Fig. 4b). At this pressure, a refinement based on Pnma-structured H_4S_3 and C2/c-structured H_3S leads to poorer fits with higher R_p and R_{wp} values (Supplemental Material, Fig. S12 [52]), which supports the existence of residual H_2S (about 1.6%).

H_4S_3 becomes metallic at 102 GPa (Supplemental Material, Fig. S14 [52]). However, the calculated electron-phonon-coupling parameter ($\lambda = 0.42$) is very small at 140 GPa due to the low density of states at the Fermi level of 0.09 eV^{-1}/atom. As a result, the T_c estimated from the Allen and Dynes modified McMillan equation [53] with μ^* of 0.16–0.13 is only 0.75–2.1 K at 140 GPa.

In Fig. 5, we compare the calculated T_c values for H_4S_3, H_2S and H_3S to experimental data measured in compressed H_2S [1], where T_c obtained for samples prepared at low and high temperatures are denoted by L-T_c and H-T_c, respectively. On the one hand, the observed L-T_c [1] at pressures below 160 GPa can only be quantitatively reproduced by H_2S, while the nature of the rapidly increasing L-T_c above 160 GPa remains unclear because the calculated T_c values of H_3S, H_4S_3, and H_2S are too high, too low, and tending to decrease, respectively. On the other hand, although the values of T_c for Im$\bar{3}$m structured H_3S calculated within the harmonic approximation are much higher than the observed H-T_c [54], the inclusion of anharmonic effects reproduces the H-T_c data above 180 GPa [35] quite well. However, at low pressures around 150 GPa, T_c values [54] estimated for R3m-H_3S within the harmonic approximation are ∼45 K lower than the observed H-T_c. Meanwhile, the predicted T_c for R3m-H_3S increases with pressure, in stark contrast to the experimental observation of a decrease in H-T_c. Apparently, further study is greatly needed to disclose the steep T_c increase of L-T_c above 160 GPa and the high H-T_c at around 150 GPa.

We find that kinetics plays an important role in determining the experimentally observed H-S structures. Theory suggests that H_2S and H_4S_3 decompose above 25 and 113 GPa (Supplemental Material Fig. S13 and Fig. 2d), respectively. However, H_2S and H_4S_3 are observed to persist up to at least 140 GPa. Large kinetic barriers must therefore play a major role in suppressing decomposition at high pressures, as has been found in other materials [55–58].

In summary, through first-principles structure searching calculations, we predict three new stable H-S compounds with stoichiometries H_3S_2, H_2S_3, and H_4S_3 and a new C2/c structure of H_3S, enriching the phase diagram of H-S systems at high pressures. The formation of H_4S_3 and H_3S was confirmed by XRD experiments to occur through decomposition of compressed H_2S above 27 GPa resulting in the products S + H_3S + H_4S_3. H_4S_3 becomes a major component at around 66 GPa and is stable up to at least 140 GPa, with a small fraction of H_3S and residual H_2S. We have also examined potential superconductivity of metallic H_4S_3 via explicit calculations of electron-phonon coupling parameters and the superconducting T_c. Our work suggests that kinetically

protected H_2S in samples prepared at low temperature is responsible for the observed superconductivity below 160 GPa.

Y. L. and J. H. acknowledge funding from the National Natural Science Foundation of China under Grant No. 11204111 and No. 11404148, the Natural Science Foundation of Jiangsu province under Grant No. BK20130223, and the PAPD of Jiangsu Higher Education Institutions. Y. Z. and Y. M. acknowledge funding from the National Natural Science Foundation of China under Grant Nos. 11274136 and 11534003, the 2012 Changjiang Scholars Program of China. R. J. N. acknowledges financial support from the Engineering and Physical Sciences Research Council (EPSRC) of the U.K. [EP/J017639/1]. Calculations were performed on the Cambridge High Performance Computing Service facility and the HECToR and Archer facilities of the U.K.'s national high-performance computing service (for which access was obtained via the UKCP consortium [EP/K013564/1]). J. R. N. acknowledges financial support from the Cambridge Commonwealth Trust. I. E. acknowledges financial support from the Spanish Ministry of Economy and Competitiveness (FIS2013-48286-C2-2-P). M. C. acknowledges support from the Graphene Flagship and Agence nationale de la recherche (ANR), Grant No. ANR-13-IS10-0003-01. Work at Carnegie was partially supported by EFree, an Energy Frontier Research Center funded by the DOE, Office of Science, Basic Energy Sciences under Award No. DE-SC-0001057 (salary support for H. L.). The infrastructure and facilities used at Carnegie were supported by NNSA Grant No. DE-NA-00006, CDAC.

* Electronic address: mym@jlu.edu.cn

[1] A. P. Drozdov, M. I. Eremets, I. A. Troyan, V. Ksenofontov, and S. I. Shylin, Nature (2015). Advance online publication, doi:10.1038/nature14964.
[2] N. W. Ashcroft, Phys. Rev. Lett. **21**, 1748 (1968).
[3] N. W. Ashcroft, Phys. Rev. Lett. **92**, 187002 (2004).
[4] C. J. Pickard and R. J. Needs, Phys. Rev. Lett. **97**, 045504 (2006).
[5] C. J. Pickard and R. J. Needs, Phys. Rev. B. **76**, 144114 (2007).
[6] G. Gao, H. Wang, A. Bergara, Y. Li, G. Liu, and Y. Ma, Phys. Rev. B **84**, 064118 (2011).
[7] R. Szcześniak and A. Durajski, Supercond. Sci. Technol. **27**, 015003 (2014).
[8] G. Gao, A. R. Oganov, P. Li, Z. Li, H. Wang, T. Cui, Y. Ma, A. Bergara, A. O. Lyakhov, T. Iitaka, and G. Zou, Proc. Nat. Acad. Sci. U.S.A. **107**, 1317 (2010).
[9] G. Gao, A. R. Oganov, A. Bergara, M. Martinez-Canales, T. Cui, T. Iitaka, Y. Ma, and G. Zou, Phys. Rev. Lett. **101**, 107002 (2008).
[10] A. P. Durajski, Eur. Phys. J. B **87**, 211 (2014).
[11] X. Jin, X. Meng, Z. He, Y. Ma, B. Liu, T. Cui, G. Zou, and H. Mao, Proc. Nat. Acad. Sci. U.S.A. **107**, 9969 (2010).
[12] Y. Li, G. Gao, Y. Xie, Y. Ma, T. Cui, and G. Zou, Proc. Nat. Acad. Sci. U.S.A. **107**, 15708 (2010).
[13] H. Wang, S. T. John, K. Tanaka, T. Iitaka, and Y. Ma, Proc. Nat. Acad. Sci. U.S.A. **109**, 6463 (2012).
[14] D. Y. Kim, R. H. Scheicher, and R. Ahuja, Phys. Rev. Lett. **103**, 077002 (2009).
[15] Y. Li, J. Hao, H. Liu, S. T. John, Y. Wang, and Y. Ma, Scientific Reports **5**, 09948 (2015).
[16] H. Shimizu, Y. Nakamichi, and S. Sasaki, J. Chem. Phys. **95**, 2036 (1991).
[17] S. Endo, N. Ichimiya, K. Koto, S. Sasaki, and H. Shimizu, Phys. Rev. B **50**, 5865 (1994).
[18] S. Endo, A. Honda, S. Sasaki, H. Shimizu, O. Shimomura, and T. Kikegawa, Phys. Rev. B **54**, R717 (1996).
[19] S. Endo, A. Honda, K. Koto, O. Shimomura, T. Kikegawa, and N. Hamaya, Phys. Rev. B **57**, 5699 (1998).
[20] H. Fujihisa, H. Yamawaki, M. Sakashita, K. Aoki, S. Sasaki, and H. Shimizu, Phys. Rev. B **57**, 2651 (1998).
[21] H. Fujihisa, H. Yamawaki, M. Sakashita, A. Nakayama, T. Yamada, and K. Aoki, Phys. Rev. B **69**, 214102 (2004).
[22] M. Sakashita, H. Yamawaki, H. Fujihisa, K. Aoki, S. Sasaki, and H. Shimizu, Phys. Rev. Lett. **79**, 1082 (1997).
[23] H. Shimizu and S. Sasaki, Science **257**, 514 (1992).
[24] H. Shimizu, H. Yamaguchi, S. Sasaki, A. Honda, S. Endo, and M. Kobayashi, Phys. Rev. B **51**, 9391 (1995).
[25] H. Shimizu, T. Ushida, S. Sasaki, M. Sakashita, H. Yamawaki, and K. Aoki, Phys. Rev. B **55**, 5538 (1997).
[26] J. Loveday, R. Nelmes, S. Klotz, J. Besson, and G. Hamel, Phys. Rev. Lett. **85**, 1024 (2000).
[27] M. Sakashita, H. Fujihisa, H. Yamawaki, and K. Aoki, The Journal of Physical Chemistry A **104**, 8838 (2000).
[28] R. Rousseau, M. Boero, M. Bernasconi, M. Parrinello, and K. Terakura, Phys. Rev. Lett. **85**, 1254 (2000).
[29] Y. Li, J. Hao, H. Liu, Y. Li, and Y. Ma, J. Chem. Phys. **140**, 174712 (2014).
[30] T. A. Strobel, P. Ganesh, M. Somayazulu, P. R. C. Kent, and R. J. Hemley, Phys. Rev. Lett. **107**, 255503 (2011).
[31] D. Duan, Y. Liu, F. Tian, D. Li, X. Huang, Z. Zhao, H. Yu, B. Liu, W. Tian, and T. Cui, Scientific Reports **4**, 6968 (2014).
[32] C. J. Pickard, M. Martinez-Canales, and R. J. Needs, Phys. Rev. Lett. **110**, 245701 (2013).
[33] N. Bernstein, C. S. Hellberg, M. D. Johannes, I. I. Mazin, and M. J. Mehl, Phys. Rev. B **91**, 060511(R) (2015).
[34] D. Duan, X. Huang, F. Tian, D. Li, H. Yu, Y. Liu, Y. Ma, B. Liu, and T. Cui, Phys. Rev. B **91**, 180502 (2015).
[35] I. Errea, M. Calandra, C. J. Pickard, J. R. Nelson, R. J. Needs, Y. Li, H. Liu, Y. Zhang, Y. Ma, and F. Mauri, Phys. Rev. Lett. **114**, 157004 (2015).
[36] Y. Wang, J. Lv, L. Zhu, and Y. Ma, Phys. Rev. B **82**, 094116 (2010).
[37] Y. Wang, J. Lv, L. Zhu, and Y. Ma, Comput. Phys. Commun. **183**, 2063 (2012).
[38] C. J. Pickard and R. J. Needs, J. Phys.: Condens. Matter **23**, 053201 (2011).
[39] L. Zhu, H. Wang, Y. Wang, J. Lv, Y. Ma, Q. Cui, Y. Ma, and G. Zou, Phys. Rev. Lett. **106**, 145501 (2011).
[40] Y. Wang, H. Liu, J. Lv, L. Zhu, H. Wang, and Y. Ma, Nat. Commun. **2**, 563 (2011).
[41] C. J. Pickard and R. J. Needs, J. Chem. Phys. **127**, 244503 (2007).
[42] C. J. Pickard and R. J. Needs, Nat. Phys. **3**, 473 (2007).
[43] J. M. McMahon and D. M. Ceperley, Phys. Rev. Lett.

106, 165302 (2011).
[44] C. J. Pickard, M. Martinez-Canales, and R. J. Needs, Phys. Rev. B **85**, 214114 (2012).
[45] Y. Li, Y. Wang, C. J. Pickard, R. J. Needs, Y. Wang, and Y. Ma, Phys. Rev. Lett. **114**, 125501 (2015).
[46] G. Kresse and J. Furthmüller, Phys. Rev. B **54**, 11169 (1996).
[47] S. J. Clark, M. D. Segall, C. J. Pickard, P. J. Hasnip, M. I. Probert, K. Refson, and M. C. Payne, Z. Kristallogr. **220**, 567 (2005).
[48] P. Giannozzi, S. Baroni, N. Bonini, M. Calandra, R. Car, C. Cavazzoni, D. Ceresoli, G. L. Chiarotti, M. Cococcioni, I. Dabo *et al*, J. Phys.: Condens. Matter **21**, 395502 (2009).
[49] A. L. Ruoff, H. Luo, C. Vanderborgh, H. Xia, K. Brister, and V. Arnold, Rev. Sci. Instrum. **64**, 3462 (1993).
[50] A. C. Larson and R. B. Von Dreele, General Structure Analysis System. LANSCE, MS-H805, Los Alamos, New Mexico (1994).
[51] B. H. Toby, J. Appl. Cryst. **34**, 210 (2001).
[52] Reserved for EPAPS.
[53] P. B. Allen and R. C. Dynes, Phys. Rev. B **12**, 905 (1975).
[54] R. Akashi, M. Kawamura, S. Tsuneyuki, Y. Nomura, and R. Arita, Phys. Rev. B **91**, 224513 (2015).
[55] A. R. Oganov, in Boron Rich Solids (Springer, 2011), pp. 207.
[56] G. Gao, A. R. Oganov, Y. Ma, H. Wang, P. Li, Y. Li, T. Iitaka, and G. Zou, J. Chem. Phys. **133**, 144508 (2010).
[57] P. Kroll, T. Schröter, and M. Peters, Angew. Chem. Int. Ed. **44**, 4249 (2005).
[58] X. Zhong, Y. Wang, F. Peng, H. Liu, H. Wang, and Y. Ma, Chemical Science **5**, 3936 (2014).